arXiv:1608.07026v1 [math.DS] 25 Aug 2016

Complex dynamics generated by negative and positive feedback delays of a prey-predator system with prey refuge: Hopf bifurcation to Chaos

Debaldev Jana[a], R. Gopal[b] and M. Lakshmanan[c]

[a] *Department of Mathematics,*
SRM University,
Kattankulathur - 603 203, Tamil Nadu, India

[b] *School of Electrical and Electronics Engineering,*
SASTRA University,
Thanjavur -613 401, Tamil Nadu, India

[c] *Centre for Nonlinear Dynamics,*
School of Physics, Bharathidasan University,
Tiruchirapalli - 620 024, India.

Abstract

Various field and laboratory experiments show that prey refuge plays a significant role in the stability of prey-predator dynamics. On the other hand, theoretical studies show that delayed system exhibits a much more realistic dynamics than its non-delayed counterpart. In this paper, we study a multi-delayed prey-predator model with prey refuge. We consider modified Holling Type II response function that incorporates the effect of prey refuge and then introduce two discrete delays in the model system. A negative feedback delay is considered in the logistic prey growth rate to represent density dependent feedback mechanism and a positive feedback delay is considered to represent the gestation time of the predator. Our study reveals that the system exhibits different dynamical behaviors, viz., stable coexistence, periodic coexistence or chaos depending on the values of the delay parameters and degree of prey refuge. The interplay between two delays for a fixed value of prey refuge has also been determined. It is noticed that these delays work in a complementary fashion. In addition, using the normal form theory and center manifold argument, we derive the explicit formulae for determining the direction of the bifurcation, the stability and other properties of the bifurcating periodic solutions.

Key words: prey-predator model, prey refuge, multiple-delay, direction and stability, Hopf bifurcation, chaos.

1 Introduction

Interaction between food and its eater is the basic rule of nature. Interrelationship [1, 2] largely depends and varies upon the structure of habitat and more prominently their habitat selection [3, 4]. Refuge means a place or state of safety [5]. The predation risk often induces the use of safer 'refuge' habitats by prey population and refuge use under predation risk is commonly observed in a wide range of systems [6, 7, 8, 9, 10, 11, 12]. Refuge habitats can change the dynamic behavior of prey-predator interaction by decreasing the predation risk [1, 3, 13]. Ray and Straškraba [15] notice that the prey species, i.e., detritivorous fish and their predator species, carnivorous fish coexist in Sundarban Mangrove ecosystem. In the pristine part of the ecosystem where forest is dense, the production of detritus is high and the detritivorous fish can easily take refuge in the densely inundated bushy part of the forest to avoid predation by carnivorous fish. In this part the production and densities of both prey and predator fish are high and coexist with each other. But in the reclaimed part of the forest where there is huge anthropogenic stress, production of detritus is less and due to lack of bushy part of the forest the area for refuge of prey species is minimum. In this reclaimed area prey density (detritivorous fish) is reduced at an alarming level but predator fish population is also slightly reduced because this fish population has switched its food habit to other fish and animals [16]. Predator's functional response is assumed to be one of the most important components of prey-predator interaction because predation intensity may change the shape of the community structure and ecosystem properties [14]. It is well established that prey refuge reduces the predation rate and the hypothesis is that there exists an inverse relationship between predation rate and degree of prey refuge [17]. Therefore, it is important to incorporate the effect of prey refuge in the predator response function when we study the prey-predator model. A generalized Gause-type prey-predator model is given by

$$\begin{aligned} \dot{x}(t) &= x(t)f(x(t)) - y(t)g(x(t)), \\ \dot{y}(t) &= \theta y(t)g(x(t)) - dy(t), \end{aligned} \tag{1.1}$$

where x and y denote the prey and predator densities, respectively. d is the death rate constant and θ is the conversion efficiency of the predator. $f(x)$ is the specific growth rate of prey in the absence of predator and $g(x)$ is the predator response function. It is shown that the most commonly used Holling Type II functional response, given by $g(x(t)) = \frac{\alpha x}{1+\alpha h x}$, can be modified to

$g(x(t)) = \frac{\alpha(1-m)x}{1+\alpha(1-m)hx}$ [18, 19, 20, 21] in the presence of prey refuge. Here α is the prey attack coefficient, h is the handling time and m $(0 < m < 1)$ is the degree or strength of prey refuge. For example, $m = 0.30$ implies that prey-predator interaction will be reduced by 30% due to prey refuge. If $m = 0$, i.e. in the absence of prey refuge, it will be exactly the Holling Type II response function.

Assume that the prey grows logistically to environmental carrying capacity k in the absence of predator with intrinsic growth rate r. In this case, the generalized Gause-type prey-predator model (1.1) with modified Type II response function that incorporates the effect of prey refuge takes the following form:

$$\begin{aligned} \dot{x}(t) &= rx(1 - \tfrac{x}{k}) - \tfrac{\alpha(1-m)xy}{1+\alpha(1-m)hx}, \\ \dot{y}(t) &= y\left[\tfrac{\theta\alpha(1-m)x}{1+\alpha(1-m)hx} - d\right]. \end{aligned} \tag{1.2}$$

Models with delay are much more realistic, as in reality time delays occur in almost every biological situation [25] and they are assumed to be one of the reasons for regular fluctuations in population density [26, 27]. Assuming that reproduction of predator after consuming prey is not instantaneous but mediated by some time lag required for gestation, we considered a delay in the predator's numerical response of the above model and determined the critical value of the delay parameter below which the system was stable and above which it was unstable [22, 20, 23, 21]. Recently, many researchers have studied the prey-predator interaction with two delays [20, 21, 28, 29, 30, 31, 32, 33]. In [28], the authors study a Lotka-Volterra prey-predator system with two delays. Considering the sum of the two delays as a bifurcation parameter, they show that the system undergoes a Hopf bifurcation when the total delay exceeds some critical value. They also determine the direction and stability of the bifurcating periodic solutions. Song et al. [29] study exactly the same model with additional analysis of global existence of periodic solutions. Nakaoka et al. [30] and Xu et al. [31] study similar type of Lotka-Volterra prey-predator model with two delays. It is to be mentioned that these studies [28, 29, 30, 31] consider the predator's functional response as Holling Type I and treat total delay as the bifurcation parameter where as stability and bifurcation analysis of a diffusive prey-predator system in Holling type III functional response with prey refuge is studied by [34]. Diffusive prey-predator system with constant prey refuge and delay is studied by [35] and on the same type system with hyperbolic

mortality is studied by [36]. A three-species prey-predator system with two delays is studied in [32]. By choosing the sum of two delays as a bifurcation parameter, the authors show that a Hopf bifurcation at the positive equilibrium of the system can occur as the total delay crosses some critical values and then determine the direction and stability of the bifurcating periodic solutions. Depending only on a single phase diagram, Nakoka et al. [30] and Liao et al. [32] comment that large delay may cause chaos. To know the effect of multi-delays on the qualitative behavior of prey-predator system with prey refuge, we modify the system (1.2) with two discrete delays. One discrete delay τ_1 is considered in the specific growth rate of prey to incorporate the effect of density dependent feedback mechanism which takes τ_1 units of time to respond to changes in the prey population [37]. The second delay τ_2 is considered in the predator response function and it is regarded as gestation period or reaction time of the predator [38]. We thus obtain the following multi-delayed prey-predator model in the presence of prey refuge as

$$\begin{aligned} \dot{x}(t) &= rx\left(1 - \tfrac{x(t-\tau_1)}{k}\right) - \tfrac{\alpha(1-m)xy}{1+\alpha(1-m)hx}, \\ \dot{y}(t) &= y\left[\tfrac{\theta\alpha(1-m)x(t-\tau_2)}{1+\alpha(1-m)hx(t-\tau_2)} - d\right]. \end{aligned} \tag{1.3}$$

All parameters are assumed to be positive. The model system (1.3) has to be investigated with initial conditions

$$x(\phi) = x_0 = \phi_1(\phi) > 0,\ y(\phi) = y_0 = \phi_1(\phi) > 0 \text{ for } \phi \in [-\max\{\tau_1, \tau_2\}, 0]. \tag{1.4}$$

The objective of our paper is to study the prey-predator dynamics in the presence of prey refuge and two biological delays. We address the question how the gestation delay τ_2 of the predator affects individually and jointly with the delay τ_1 in the logistic prey growth rate on the local stability of a prey-predator system with prey refuge. Another important issue that will be discussed is – how the system behaves if the biological delays are large enough. Existence of chaos, if any, due to large delay will be investigated rigorously. The interplay between the degree of prey refuge and biological delays will also be investigated in detail.

The organization of the paper is as follows: In Section 2, we study the local stability of the system (1.3); direction and stability of Hopf bifurcation is studied in Section 3. Rigorous numerical simulations of the model system

are performed in Section 4. Finally, a summary is presented in Section 5.

2 Stability Analysis

2.1 Positive Invariance

Feasibility or biological positivity studies aim to objectively and rationally uncover the strengths and weaknesses of an existing or proposed model in the given environment. Therefore, it is important to show the positivity for the model system (1.3) as the system represents prey-predator populations. Biologically, positivity ensures that the population never becomes negative and it always survives. For proving this, we have the following theorem.

Theorem 2.1. *All the solution of (1.3) with initial conditions (1.4) are positive.*

Proof. The model (1.3) can be written in the following form:

$$\text{Consider } W = col(x, y) \in \Re^2_+, (\phi_1(\theta), \phi_2(\theta)) \in C_+ = ([-\max\{\tau_1, \tau_2\}, 0], \Re^2_+),$$
$$\phi_1(0), \phi_2(0) > 0,$$

$$\begin{aligned} F(W) &= \begin{pmatrix} F_1(W) \\ F_2(W) \end{pmatrix} \\ &= \begin{pmatrix} x\left[r\left(1 - \dfrac{x(t-\tau_1)}{K}\right) - \dfrac{\alpha(1-m)y}{ay + (1-m)x}\right] \\ y\left[\dfrac{\theta\alpha(1-m)x(t-\tau_2)}{1 + \alpha(1-m)hx(t-\tau_2)} - d\right] \end{pmatrix}, \end{aligned}$$

model system (1.3) becomes

$$\dot{W} = F(W), \tag{1.3a}$$

with $W(\phi) = (\phi_1(\phi), \phi_2(\phi)) \in C_+$ and $\phi_1(0), \phi_2(0) > 0$. It is easy to check in system (1.3a) that whenever choosing $W(\phi) \in \Re_+$ such that $x = y = 0$, then

$$F_i(W) \mid_{w_i=0, W \in \Re_+^2} \geq 0,$$

with $w_1(t) = x(t), w_2(t) = y(t)$. Using the lemma given in [44], any solution of (1.3a) with $W(\theta) \in C_+$, say $W(t) = W(t, W(\theta))$, is such that $W(t) \in \Re_+^2$ for all $t \geq 0$. Hence the solution of the system (1.3a) exists in the region $\Re_+^2$ and all solutions remain non-negative for all $t > 0$. Therefore, the positive orthant $\Re_+^2$ is an invariant region.

2.2 Uniform persistence

In ecology, one question arises that the determining conditions which assure that the population abundance with time i.e., the solutions of the corresponding ecological system which are initially strictly positive do not approach the boundary of the cone as time evolves. Generally speaking, the uniformly persistent systems are those in which strictly positive solutions do not approach the boundary of the non-negative phase-space ($\Re_+^2$) as $t \to \infty$ [39]. In other words, permanently coexistence (uniform persistence) implies the existence of a region in the phase space at a non-zero distance from the boundary, in which all the population vectors must lie ultimately. The uniform persistence is also most suitable from the point of applications since it rules out the possibility of one of the populations becoming arbitrarily close to zero and hence the risk of extinction due to small perturbation due to stochastic effects. The concept of uniform persistence has been discussed by many researchers [40, 41, 42]. In the next theorem, we prove the uniform persistence of the the model system (1.3) by means of the well known average Lyapunov function [43].

Theorem 2.2. *The model system (1.3) is uniformly persistent if all the non-interior equilibrium points exist together with* (i) $\frac{\beta_1}{\beta_2} > \frac{d}{r}$, (ii) $m < 1 - \frac{d}{\alpha k(\theta - hd)}$, $\theta > hd + \frac{d}{\alpha k}$.

Proof The system (1.3) has two boundary equilibrium points, $(i)E_0(0,0)$ and $(ii)E_1(k,0)$. For $(x,y) \in \Re_+^2$, consider the following average Lyapunov function.

$$\rho(x,y,z) = x^{\beta_1} y^{\beta_2},$$

where $\beta_i > 0$, $i = 1, 2$ are constants. It is easy to observe that the function $\rho(.)$ is a non-negative continuous function. Calculating the logarithmic derivative of $\rho(.)$ along solution of the model system (1.3), we obtain

$$\begin{aligned}\Upsilon(x,y,z) &= \frac{\dot{\rho}}{\rho} = \frac{\beta_1 \dot{x}}{x} + \frac{\beta_2 \dot{y}}{y} \\ &= \beta_1\Big[r\bigg(1 - \frac{x(t-\tau_1)}{k} - \frac{\alpha(1-m)y}{1+\alpha(1-m)hx}\bigg)\Big] + \beta_2\Big[\frac{\theta\alpha(1-m)x(t-\tau_2)}{1+\alpha(1-m)hx(t-\tau_2)} - d\Big].\end{aligned}$$

To prove the system (1.3) to be uniformly persistent, we need to show that the above logarithmic derivative is positive at all the boundary equilibrium points E_0 and E_1 for some suitable choices of positive β_i's. This condition is ensured at the origin and axial equilibria E_0 and E_1 by the choice $\frac{\beta_1}{\beta_2} > \frac{d}{r}$, $m < 1 - \frac{d}{\alpha k(\theta - hd)}$ and $\theta > hd + \frac{d}{\alpha k}$ respectively.

2.3 Local stability

Ecological stability can refer to types of stability in a continuum ranging from regeneration via resilience (returning quickly to a previous state), to constancy to persistence. The precise definition depends on the ecosystem in question, the variable or variables of interest, and the overall context. In the context of conservation ecology, stable populations are often defined as ones that do not go extinct. Researchers applying mathematical models from system dynamics usually use Lyapunov stability. Local stability indicates that a system is stable over small short-lived disturbances. In ecology, stress is given on the stability of coexistence of equilibrium points. We, therefore, concentrate on the study of the interior equilibrium point of the system (1.3). This system has only one interior equilibrium point given by $E^*(x^*, y^*)$, where $x^* = \frac{d}{\alpha(1-m)(\theta - hd)}$ and $y^* = \frac{r(k-x^*)\{1+\alpha h(1-m)x^*\}}{\alpha k(1-m)}$. The equilibrium point will be feasible if

$$\begin{aligned}&(i)\ m < 1 - \tfrac{d}{\alpha k(\theta - hd)} \quad \text{and} \\ &(ii)\ \theta > hd + \tfrac{d}{\alpha k}.\end{aligned}$$

Linearizing the system (1.3) at (x^*, y^*), we get

$$\begin{aligned}\dot{x}(t) &= \tfrac{\alpha^2(1-m)^2hx^*y^*}{\{1+\alpha(1-m)hx^*\}^2}x(t) - \tfrac{\alpha(1-m)x^*}{1+\alpha(1-m)hx^*}y(t) - \tfrac{rx^*}{k}x(t-\tau_1), \\ \dot{y}(t) &= \tfrac{\theta\alpha(1-m)y^*}{\{1+\alpha(1-m)hx^*\}^2}x(t-\tau_2).\end{aligned} \tag{2.1}$$

The characteristic equation of the corresponding variational matrix is given by

$$\lambda^2 + A\lambda + B\lambda e^{-\lambda\tau_1} + Ce^{-\lambda\tau_2} = 0, \tag{2.2}$$

where

$$A = -\frac{\alpha^2(1-m)^2hx^*y^*}{\{1+\alpha(1-m)hx^*\}^2}\ (<0),\quad B = \frac{rx^*}{k}\ (>0)\ \text{ and }\ C = \frac{\theta\alpha^2(1-m)^2x^*y^*}{\{1+\alpha(1-m)hx^*\}^3}\ (>0).$$

One can consider several subcases. They are as follows,

2.4 Case I: $\tau_1 = 0$ and $\tau_2 = 0$

In the absence of all delays, the characteristic equation (2.2) becomes

$$\lambda^2 + (A+B)\lambda + C = 0. \tag{2.3}$$

All roots of the equation (2.3) will have negative real parts and the corresponding non-delayed system of the delay-induced system (1.3) will be locally asymptotically stable around E^* if and only if

$$(H_1)\quad A + B > 0\ \text{ and }\ C > 0.$$

Note that C is always positive whenever E^* exists and $A + B > 0$ if

$$m > 1 - \frac{\theta+hd}{\alpha kh(\theta-hd)} \text{ with } \theta > \frac{hd(1+\alpha kh)}{\alpha kh-1} \text{ and } \alpha > \frac{1}{kh}.$$

Thus, we state the following lemma for the stability of the non-delayed system.

Lemma 2.1. The system (1.3) is locally asymptotically stable around E^* in the absence of delay if

$$\begin{aligned}&(i)\ \alpha > \tfrac{1}{kh},\\ &(ii)\ \theta > \max\big[\tfrac{hd(\alpha kh+1)}{\alpha kh-1}, hd + \tfrac{d}{\alpha k}\big] \text{ and}\\ &(iii)\ 1 - \tfrac{\theta+hd}{\alpha kh(\theta-hd)} < m < 1 - \tfrac{d}{\alpha k(\theta-hd)}.\end{aligned}$$

2.5 Case II: $\tau_1 = 0$ and $\tau_2 \neq 0$

If $\tau_1 = 0$ and $\tau_2 > 0$ then the characteristic equation (2.2) becomes

$$\lambda^2 + (A+B)\lambda + Ce^{-\lambda\tau_2} = 0 \tag{2.4}$$

Let $i\omega$ ($\omega > 0$) be a root of the equation (2.4). Then it follows that

$$\begin{aligned} \omega^2 &= C\cos\omega\tau_2, \\ (A+B)\omega &= C\sin\omega\tau_2. \end{aligned} \tag{2.5}$$

This leads to

$$\omega^4 + (A+B)^2\omega^2 - C^2 = 0. \tag{2.6}$$

If Lemma 2.1 holds, then the equation (2.6) has a unique positive root ω_0^2. Substituting ω_0^2 into (2.5), we have

$$\tau_{2_n} = \frac{1}{\omega_0}\cos^{-1}\left(\frac{\omega_0^2}{C}\right) + \frac{2n\pi}{\omega_0},\ n = 0, 1, 2, ...$$

If $\lambda(\tau_2)$ be the root of (2.4) satisfying $Re\lambda(\tau_{2_n}) = 0$ and $Im\lambda(\tau_{2_n}) = \omega_0$, we get

$$\left[\frac{d}{d\tau_2}Re(\lambda)\right]_{\tau_2=\tau_{2_0},\omega=\omega_0} = \frac{2\omega^2+(A+B)^2}{C^2} > 0.$$

From Corollary (2.4) in Ruan and Wei [45], we have the following conclusions.

Lemma 2.2. Assume $\tau_1 = 0$ and conditions of Lemma 2.1 hold. Then the interior equilibrium E^* of the system (1.3) is asymptotically stable for $\tau_2 < \tau_{2_0}$ and unstable for $\tau_2 > \tau_{2_0}$. Furthermore, the system (1.3) undergoes a Hopf bifurcation at E^* when $\tau_2 = \tau_{2_0}$.

2.6 Case III: $\tau_1, \tau_2 \neq 0$ & τ_2 is within its stable range

In this case, we consider equation (2.2) with τ_2 in its stable interval and regard τ_1 as a parameter. Without loss of generality, we consider that the system (2.2) satisfies conditions of the Lemma 2.1. Let $i\omega(\omega > 0)$ be a root of equation (2.2) and thus we obtain

$$\omega^4 + \widetilde{A}\omega^2 + C^2 + 2\widetilde{B}\cos\omega\tau_2 + 2\widetilde{C}\sin\omega\tau_2 = 0. \tag{2.7}$$

where,

$$\widetilde{A} = A^2 - B^2,\quad \widetilde{B} = -C\omega^2 \text{ and } \quad \widetilde{C} = -AC\omega.$$

We define,

$$F(\omega) = \omega^4 + \widetilde{A}\omega^2 + C^2 + 2\widetilde{B}\cos\omega\tau_2 + 2\widetilde{C}\sin\omega\tau_2.$$

Then it is easy to check that $F(0) = C^2 > 0$ and $F(\infty) = \infty$. We can obtain that equation (2.7) has finite positive roots $\omega_1, \omega_2, ..., \omega_k$. For every fixed $\omega_i, i = 1, 2, ..., k$, there exists a sequence $\{\tau_{1_i}^j \mid j = 1, 2, ...\}$, where

$$\tau_{1_i}^j = \frac{1}{\omega_1}\cos^{-1}\left[\frac{C\ \sin\omega_1\tau_2 - A\omega_1}{B\omega_1}\right] + \frac{2i\pi}{\omega_1}, \quad i = 1, 2, ..., k,\ j = 1, 2, ...$$

such that (2.7) holds. Let $\tau_{1_0} = \min\{\tau_{1_i}^j \mid i = 1, 2, ..., k; j = 1, 2, ...\}$. When $\tau_1 = \tau_{1_0}$, equation (2.2) has a pair of purely imaginary roots $\pm i\omega_1$ for $\tau_2 \in [0, \tau_{2_0})$.

In the following, we assume that

$$(H_2) \qquad \left[\frac{d}{d\tau_1}(Re\lambda)\right]_{\lambda=i\omega_1} \neq 0.$$

Therefore, by the general Hopf bifurcation theorem for FDEs, we have the following result on the stability and bifurcation of the system equation (1.3).

Lemma 2.3. For the model system (1.3), suppose conditions of the Lemma 2.1 are satisfied when $\tau_2 \in [0, \tau_{2_0})$. Then the equilibrium E^* is locally asymptotically stable when $\tau_1 \in (0, \tau_{1_0})$ and unstable if $\tau_1 > \tau_{1_0}$. The system (1.3) undergoes a Hopf bifurcation at E^* when $\tau_1 = \tau_{1_0}$.

2.7 Case IV: $\tau_2 = 0$ and $\tau_1 \neq 0$

For this choice of the delay parameters we summarize our results in the following theorem. The proof follows similar arguments as the Lemma 2.2. in Cases II.

Lemma 2.4. Assume that $\tau_2 = 0, \tau_1 \neq 0$ and the condition of Lemma 2.1. hold. Then the equilibrium E^* is locally asymptotically stable for $\tau_1 < \bar{\tau}_{1_0}$ and unstable for $\tau_1 > \bar{\tau}_{1_0}$. Furthermore, the system (1.3) undergoes Hopf-bifurcation when $\tau_1 = \bar{\tau}_{1_0}$, where

$$\bar{\tau}_{1_0} = \frac{1}{\bar{\omega}_0}\cos^{-1}(-\frac{A}{B}),$$

where, $\bar{\omega}_0$ is the unique positive root of $\omega^4 + (A^2 - B^2 - 2C)\omega^2 + C^2 = 0$ and

$$\left[\frac{d(\mathrm{Re}\lambda(\tau))}{d\tau}\right]^{-1}_{\tau=\bar{\tau}} = \frac{M + 2\bar{\omega}^2}{B^2\bar{\omega}^2} > 0,$$

since $M = A^2 - B^2 - 2C = [\frac{rd\{\alpha h(1-m)(k-2x^*)-1\}}{\alpha\theta k(1-m)}]^2 > 0$.

2.8 Case V: $\tau_1, \tau_2 \neq 0$ & τ_1 is within its stable range

For this choice of the delay parameters we summarize our results in the following theorem. The proof follows similar arguments as the Lemma 2.3. in Cases III.

Lemma 2.5. For the model system (1.3), suppose conditions of the Lemma 2.1 are satisfied and $\tau_1 \in [0, \bar{\tau}_{1_0})$. Then the equilibrium E^* is locally asymptotically stable when $\tau_2 \in (0, \bar{\tau}_{2_0})$ and unstable if $\tau_2 > \bar{\tau}_{2_0}$. The system (1.3) undergoes a Hopf bifurcation at E^* when $\tau_2 = \bar{\tau}_{2_0}$, where

$$\bar{\tau}_{2_0} = \frac{1}{\bar{\omega}_1}\cos^{-1}\left(\frac{\bar{\omega}_1^2 - B\bar{\omega}_1\sin\bar{\omega}_1\tau_1}{C}\right),$$

where, $\bar{\omega}_1 > 0$ is the positive root of

$$\omega^4 + \bar{A}\omega^2 - C^2 + a\bar{C}\sin\omega\tau_1 + \bar{D}\cos\omega\tau_1 = 0,$$

with $\bar{A} = A^2 + B^2,\ \bar{B} = -B\omega^3$ and $\bar{C} = AB\omega^2$.

In the following, we also assume that

$$(H_3) \qquad \left[\frac{d}{d\tau_2}(Re\lambda)\right]_{\lambda=i\bar{\omega}_1} \neq 0.$$

3 Direction and stability of Hopf bifurcation point

In the previous section, we have obtained the sufficient conditions to guarantee that the system (1.3) undergoes Hopf bifurcation at E^* when $\tau_1 = \tau_{1_0} = \widetilde{\tau}_1$ and $\omega_1 = \widetilde{\omega}$ (say) and τ_2 is within its stability range. In this section, we study its bifurcation properties. The method we use is based on the normal form and the center manifold theory presented in Hassard et al. [46].

Without loss of generality, we assume that $\widetilde{\tau}_2 < \tau_{2_0}$, where $\widetilde{\tau}_2 \in (0, \tau_{2_0})$. Let $x_1 = x - x^*,\ x_2 = y - y^*$ and $\tau_1 = \widetilde{\tau}_1 + \mu$ where $\mu \in R$. Then equation (1.3) is transformed into an FDE in $C = C([-1, 0], R^2)$ as

$$\dot{x}(t) = L_\mu(x_t) + f(\mu, x_t). \tag{4.1}$$

Here $x(t) = (x_1, x_2)^T \in R^2$, and $L_\mu : C \to R,\ f : R \times C \to R$ are given by

$$L_\mu(\phi) = (\widetilde{\tau}_1+\mu)B_1 \begin{pmatrix} \phi_1(0) \\ \phi_2(0) \end{pmatrix} + (\widetilde{\tau}_1+\mu)B_2 \begin{pmatrix} \phi_1(-\widetilde{\tau}_1) \\ \phi_2(-\widetilde{\tau}_1) \end{pmatrix} + (\widetilde{\tau}_1+\mu)B_3 \begin{pmatrix} \phi_1(-\widetilde{\tau}_2) \\ \phi_2(-\widetilde{\tau}_2) \end{pmatrix} \quad (4.2)$$

with $B_1 = \begin{pmatrix} \frac{\alpha^2(1-m)^2 h x^* y^*}{\{1+\alpha(1-m)hx^*\}^2} & -\frac{\alpha(1-m)x^*}{1+\alpha(1-m)hx^*} \\ 0 & 0 \end{pmatrix}$, $B_2 = \begin{pmatrix} -\frac{rx^*}{k} & 0 \\ 0 & 0 \end{pmatrix}$, $B_3 = \begin{pmatrix} 0 & 0 \\ \frac{\theta\alpha(1-m)y^*}{\{1+\alpha(1-m)hx^*\}^2} & 0 \end{pmatrix}$

and

$$f(\mu, \phi) = (\widetilde{\tau}_1 + \mu) \begin{pmatrix} -\frac{r}{k}\phi_1(0)\phi_1(-\widetilde{\tau}_1) - \frac{\alpha(1-m)\phi_1(0)\phi_2(0)}{1+\alpha(1-m)h\phi_1(0)} \\ \frac{\theta\alpha(1-m)\phi_1(-\widetilde{\tau}_2)\phi_2(0)}{1+\alpha(1-m)h\phi_1(-\widetilde{\tau}_2)} \end{pmatrix}. \quad (4.3)$$

By Riesz representation theorem, there exits a function $\eta(\vartheta, \mu)$ of bounded variation for $\vartheta \in [-1, 0]$ such that

$$L_\mu\phi = \int_{-1}^{0} d\eta(\vartheta, \mu)\phi(\vartheta) \quad \text{for } \phi \in C. \quad (4.4)$$

In fact, we can choose

$$\eta(\vartheta, \mu) = \begin{cases} (\widetilde{\tau}_1 + \mu)B_1, & \vartheta = 0, \\ (\widetilde{\tau}_1 + \mu)B_2\delta(\vartheta + \widetilde{\tau}_1), & \vartheta \in [-\widetilde{\tau}_1, 0), \\ -(\widetilde{\tau}_1 + \mu)B_3\delta(\vartheta + \widetilde{\tau}_2), & \vartheta \in [-\widetilde{\tau}_2, -\widetilde{\tau}_1). \end{cases} \quad (4.5)$$

For $\phi \in C^1([-1, 0], R^2)$, we define

$$A(\mu)\phi = \begin{cases} \dfrac{d\phi(\vartheta)}{d\vartheta}, & \vartheta \in [-\widetilde{\tau}_2, 0), \\ \int_{-1}^{0} d\eta(\mu, s)\phi(s), & \vartheta = 0, \end{cases}$$

and

$$R(\mu)\phi = \begin{cases} 0, & \vartheta \in [-\widetilde{\tau}_2, 0) \\ f(\mu, \phi), & \vartheta = 0. \end{cases}$$

Then system (4.1) is equivalent to

$$\dot{x}(t) = A(\mu)x_t + R(\mu)x_t, \quad (4.6)$$

where $x_t(\vartheta) = x(t + \vartheta) \quad for \quad \vartheta \in [-1, 0]$.
For $\psi \in C^1([0, -1], (R^2)^*)$, define

$$A^*\psi(s) = \begin{cases} -\dfrac{d\psi(s)}{ds}, & s \in (0, 1], \\ \int_{-1}^{0} d\eta^T(t, 0)\psi(-t), & s = 0, \end{cases}$$

and a bilinear inner product

$$\langle \psi(s), \phi(\vartheta) \rangle = \overline{\psi}(0)\phi(0) - \int_{-1}^{0} \int_{\xi=0}^{\vartheta} \overline{\psi}(\xi - \vartheta) d\eta(\vartheta)\phi(\xi) d\xi, \qquad (4.7)$$

where $\eta(\vartheta) = \eta(\vartheta, 0)$. Then A(0) and A^* are adjoint operators. From Section 2, we know that $\pm i\widetilde{\omega}\widetilde{\tau}_1$ are eigenvalues of A(0). Thus, they are also eigenvalues of A^*. We first need to compute the eigenvalues of A(0) and A^* corresponding to $i\widetilde{\omega}\widetilde{\tau}_1$ and $-i\widetilde{\omega}\widetilde{\tau}_1$, respectively. Suppose that $q(\vartheta) = (1, q_1)^T e^{i\widetilde{\omega}\widetilde{\tau}_1\vartheta}$ is the eigenvector of A(0) corresponding to $i\widetilde{\omega}\widetilde{\tau}_1$, then $A(0)q(\vartheta) = i\widetilde{\omega}\widetilde{\tau}_1 q(\vartheta)$. It follows from the definition of A(0) and (4.2), (4.4), (4.5) that

$$\widetilde{\tau}_1 \begin{pmatrix} i\widetilde{\omega} - \frac{\alpha^2(1-m)^2 hx^* y^*}{\{1+\alpha(1-m)hx^*\}^2} + \frac{rx^* e^{-i\widetilde{\omega}\widetilde{\tau}_1}}{k} & \frac{\alpha(1-m)x^*}{1+\alpha(1-m)hx^*} \\ -\frac{\theta\alpha(1-m)y^* e^{-i\widetilde{\omega}\widetilde{\tau}_2}}{\{1+\alpha(1-m)hx^*\}^2} & i\widetilde{\omega} \end{pmatrix} q(0) = \begin{pmatrix} 0 \\ 0 \end{pmatrix}.$$

Thus, we can easily obtain

$$q(0) = (1, q_1)^T,$$

where

$$q_1 = \frac{\theta\alpha(1-m)y^* e^{-i\widetilde{\omega}\widetilde{\tau}_2}}{i\widetilde{\omega}\{1+\alpha(1-m)hx^*\}^2}.$$

Similarly, let $q^*(s) = D(1, {q_1}^*)^T$ is the eigenvector of A^* corresponding to $-i\widetilde{\omega}\widetilde{\tau}_1$. By the definition of A^* and (4.2),(4.3) and (4.4), we can compute

$$q^*(s) = D(1, {q_1}^*) = D\left(1, -\frac{\alpha(1-m)x^*}{i\widetilde{\omega}\{1+\alpha(1-m)hx^*\}}\right).$$

In order to assure $\langle q^*(s), q(\vartheta) \rangle = 1$, we need to determine the value of D. From (4.7), we have

$$\begin{aligned} \langle q^*(s), q(q_1) \rangle &= \overline{D}(1, \overline{q_1}^*)(1, q_1)^T - \int_{-\widetilde{\tau}_2}^{0} \int_{\xi=0}^{\vartheta} \overline{D}(1, \overline{q_1}^*) e^{-i\widetilde{\omega}(\xi-\vartheta)} d\eta(\vartheta)(1, q_1)^T e^{i\widetilde{\omega}\xi} d\xi \\ &= \overline{D}\left\{ \left(1 - \frac{rx^*}{K} e^{-i\widetilde{\omega}\widetilde{\tau}_1}\right) + q_1 q_1^* \left(1 + \frac{\theta\alpha(1-m)y^* e^{-i\widetilde{\omega}\widetilde{\tau}_2}}{\{1+\alpha(1-m)hx^*\}^2}\right) \right\}. \end{aligned}$$

Thus, we can choose D as

$$\overline{D} = \frac{1}{\left(1 - \frac{rx^*}{K} e^{-i\widetilde{\omega}\widetilde{\tau}_1}\right) + q_1 q_1^* \left(1 + \frac{\theta\alpha(1-m)y^* e^{-i\widetilde{\omega}\widetilde{\tau}_2}}{\{1+\alpha(1-m)hx^*\}^2}\right)}.$$

In the remainder of the section, we use the same notations as in [47]. We first compute the coordinates to describe the center manifold C_0 at $\mu = 0$. Define

$$z(t) = \langle q^*, x_t \rangle, \qquad W(t,\vartheta) = x_t(\vartheta) - 2\mathrm{Re}\{z(t)q(\vartheta)\}. \tag{4.8}$$

On the center manifold C_0, we have

$$W(t,\vartheta) = W(z(t), \overline{z}(t), \vartheta),$$

where

$$W(z,\overline{z},\vartheta) = W_{20}(\vartheta)\frac{z^2}{2} + W_{11}(\vartheta)z\overline{z} + W_{02}(\vartheta)\frac{\overline{z}^2}{2} + W_{30}(\vartheta)\frac{z^3}{6} + ..., \tag{4.9}$$

z and $\overline{z}$ are local coordinates for center manifold C_0 in the direction of q^* and $\overline{q}^*$. Note that W is real if x_t is real. We only consider real solutions. For solution $x_t \in C_0$ of (4.6), since $\mu = 0$, we have

$$\dot{z}(t) = i\widetilde{\omega}\widetilde{\tau}_1 z + \overline{q}^*(\vartheta) f(0, W(z,\overline{z},\vartheta) + 2\mathrm{Re}\{zq(\vartheta)\}) \stackrel{\text{def}}{=\!=} i\widetilde{\omega}\widetilde{\tau}_1 z + \overline{q}^*(0) f_0(z,\overline{z}).$$

We rewrite this equation as

$$\dot{z}(t) = i\widetilde{\omega}\widetilde{\tau}_1 z(t) + g(z,\overline{z}),$$

where

$$g(z,\overline{z}) = \overline{q}^*(0) f_0(z,\overline{z}) = g_{20}\frac{z^2}{2} + g_{11}z\overline{z} + g_{02}\frac{\overline{z}^2}{2} + g_{21}\frac{z^2\overline{z}}{2} + ... \tag{4.10}$$

It follows from (4.8) and (4.9) that

$$\begin{aligned} x_t(\vartheta) &= W(t,\vartheta) + 2\mathrm{Re}\{z(t)q(t)\} \\ &= W_{20}(\vartheta)\frac{z^2}{2} + W_{11}(\vartheta)z\overline{z} + W_{02}(\vartheta)\frac{\overline{z}^2}{2} + (1, q_1)^T e^{i\widetilde{\omega}\widetilde{\tau}_1\vartheta} z \\ &+ (1, \overline{q_1})^T e^{-i\widetilde{\omega}\widetilde{\tau}_1\vartheta}\overline{z} + ... \end{aligned} \tag{4.11}$$

It follows together with (4.3) that

$$
\begin{aligned}
g(z,\overline{z}) &= \overline{q}^*(0)f(0,x_t) = \widetilde{\tau}_1\overline{D}(1,\overline{q_1}^*)\begin{pmatrix} -\frac{r}{k}x_{1t}(0)x_{1t}(-\widetilde{\tau}_1)-\frac{\alpha(1-m)x_{1t}(0)x_{2t}(0)}{1+\alpha(1-m)hx_{1t}(0)} \\ \frac{\theta\alpha(1-m)x_{1t}(-\widetilde{\tau}_2)x_{2t}(0)}{1+\alpha(1-m)hx_{1t}(-\widetilde{\tau}_2)} \end{pmatrix} \\
&= -\frac{\widetilde{\tau}_1 r\overline{D}}{k}[z^2e^{-i\widetilde{\omega}\widetilde{\tau}_1}+\overline{z}^2e^{i\widetilde{\omega}\widetilde{\tau}_1}+(e^{i\widetilde{\omega}\widetilde{\tau}_1}+e^{-i\widetilde{\omega}\widetilde{\tau}_1})z\overline{z}+\{2(W_{11}^1(-\widetilde{\tau}_1)+W_{11}^1(0)e^{-i\widetilde{\omega}\widetilde{\tau}_1}) \\
&+ W_{20}^1(-\widetilde{\tau}_1)+W_{20}^1(0)e^{i\widetilde{\omega}\widetilde{\tau}_1}\}\frac{z^2\overline{z}}{2}] - \widetilde{\tau}_1\overline{D}\alpha(1-m)[q_1z^2+\overline{q_1z}^2+(q_1+\overline{q_1})z\overline{z} \\
&+ \frac{z^2\overline{z}}{2}\{2(q_1W_{11}(0)+W_{11}^2(0))+(\overline{q_1}W_{20}^1(0)+W_{20}^2(0))\}] \\
&+ 2\widetilde{\tau}_1\overline{D}\alpha^2(1-m)^2h(\overline{q_1}+2q_1)\frac{z^2\overline{z}}{2}+\widetilde{\tau}_1\overline{D\overline{q_1^*}}\theta\alpha(1-m)[q_1e^{-i\widetilde{\omega}\widetilde{\tau}_2}z^2+\overline{q_1}e^{i\widetilde{\omega}\widetilde{\tau}_2}\overline{z}^2 \\
&+ (\overline{q_1}e^{-i\widetilde{\omega}\widetilde{\tau}_2}+q_1e^{i\widetilde{\omega}\widetilde{\tau}_2})z\overline{z}+\{2(W_{11}^2(0)e^{-i\widetilde{\omega}\widetilde{\tau}_2}+W_{11}^1(-\widetilde{\tau}_2)q_1) \\
&+ (W_{20}^2)(0)e^{i\widetilde{\omega}\widetilde{\tau}_2}+\overline{q_1}W_{20}^1(-\widetilde{\tau}_2)\}\frac{z^2\overline{z}}{2}] \\
&- 2\widetilde{\tau}_1\overline{D\overline{q_1^*}}\theta\alpha^2(1-m)^2h(\overline{q_1}e^{-2i\widetilde{\omega}\widetilde{\tau}_2}+2q_1)\frac{z^2\overline{z}}{2}..... \qquad (4.12)
\end{aligned}
$$

Comparing the coefficients with (4.10), we have

$$
\begin{aligned}
g_{20} &= 2\widetilde{\tau}_1\overline{D}[-\frac{r}{k}e^{-i\widetilde{\omega}\widetilde{\tau}_1}+\alpha(1-m)q_1(\theta\overline{q_1}^*e^{-i\widetilde{\omega}\widetilde{\tau}_2}-1)], \\
g_{11} &= 2\widetilde{\tau}_1\overline{D}[-\frac{r}{k}(e^{i\widetilde{\omega}\widetilde{\tau}_1}+e^{-i\widetilde{\omega}\widetilde{\tau}_1})+\alpha(1-m)\{\theta\overline{q_1}^*(\overline{q_1}e^{-i\widetilde{\omega}\widetilde{\tau}_2}+q_1e^{i\widetilde{\omega}\widetilde{\tau}_2})-Re\{q_1\}\}], \\
g_{02} &= 2\widetilde{\tau}_1\overline{D}[-\frac{r}{k}e^{i\widetilde{\omega}\widetilde{\tau}_1}+\alpha(1-m)\overline{q_1}(\theta\overline{q_1}^*e^{i\widetilde{\omega}\widetilde{\tau}_2}-1)], \\
g_{21} &= -\frac{\widetilde{\tau}_1 r\overline{D}}{k}\{2(W_{11}^1(-\widetilde{\tau}_1)+W_{11}^2(0)e^{-i\widetilde{\omega}\widetilde{\tau}_1})+W_{20}^1(0)(-\widetilde{\tau}_1)+W_{20}^2(0)e^{i\widetilde{\omega}\widetilde{\tau}_1}\} \\
&- \widetilde{\tau}_1\overline{D}\alpha(1-m)\{2(q_1W_{11}^1(0)+W_{11}^2(0))+(\overline{q_1}W_{20}^1(0)+W_{20}^2(0))\} \\
&+ 2\widetilde{\tau}_1\overline{D}\alpha^2(1-m)^2h(\overline{q_1}+2q_1)+\widetilde{\tau}_1\overline{D}\overline{q_1}^*\theta\alpha(1-m)\{W_{11}^2(0)e^{-i\widetilde{\omega}\widetilde{\tau}_2}+W_{11}^1(-\widetilde{\tau}_2q_1) \\
&+ (W_{20}^2(0)e^{i\widetilde{\omega}\widetilde{\tau}_2}+\overline{q_1}W_{20}^1(-\widetilde{\tau}_2))\}-2\widetilde{\tau}_1\overline{D}\overline{q_1}^*\theta\alpha^2(1-m)^2h(\overline{q_1}e^{-2i\widetilde{\omega}\widetilde{\tau}_2}+2q_1). \qquad (4.13)
\end{aligned}
$$

Since there are $W_{20}(\vartheta)$ and $W_{11}(\vartheta)$ in g_{21}, we still need to compute them.
From (4.3) and (4.8), we have

$$
\begin{aligned}
\dot{W} = \dot{x}_t - \dot{z} - \dot{\overline{z}}\overline{q} &= \begin{cases} AW - 2\mathrm{R}e\{\overline{q}^*(0)f_{0q}(\vartheta)\}, & \vartheta\in[-1,0), \\ AW - 2\mathrm{R}e\{\overline{q}^*(0)f_{0q}(\vartheta)\}+f_0, & \vartheta=0, \end{cases} \\
&\stackrel{\mathrm{def}}{=\!=} AW + H(z,\overline{z},\vartheta), \qquad (4.14)
\end{aligned}
$$

where

$$H(z,\overline{z},\vartheta) = H_{20}(\vartheta)\frac{z^2}{2} + H_{11}(\vartheta)z\overline{z} + H_{02}(\vartheta)\frac{\overline{z}^2}{2} + ... \tag{4.15}$$

Substituting the corresponding series into (4.14) and comparing the coefficients, we obtain

$$(A - 2i\widetilde{\omega}\widetilde{\tau}_1)W_{20}(\vartheta) = -H_{20}(\vartheta), \qquad AW_{11}(\vartheta) = -H_{11}(\vartheta)..... \tag{4.16}$$

From (4.14), we know that for $\vartheta \in [-1, 0)$,

$$H(z,\overline{z},\vartheta) = -\overline{q}^*(0)f_0q(\vartheta) - q^*(0)\overline{f}_0(\vartheta) = -g(z,\overline{z})q(\vartheta) - \overline{g}(z,\overline{z})\overline{q}(\vartheta), \tag{4.17}.$$

Comparing the coefficients with (4.15), we get

$$H_{20}(\vartheta) = -g_{20}q(\vartheta) - \overline{g}_{02}\overline{q}(\vartheta)$$

and

$$H_{11}(\vartheta) = -g_{11}q(\vartheta) - \overline{g}_{11}\overline{q}(\vartheta).$$

From (4.16) and (4.18) and the definition of A, it follows that

$$\dot{W}_{20}(\vartheta) = 2i\widetilde{\omega}\widetilde{\tau}_1W_{20}(\vartheta) + g_{20}q(\vartheta) + \overline{g}_{02}\overline{q}(\vartheta).$$

Notice that $q(\vartheta) = (1, x)^T e^{i\widetilde{\omega}\widetilde{\tau}_1\vartheta}$, hence

$$W_{20}(\vartheta) = \frac{ig_{20}}{\widetilde{\omega}}q(0)e^{i\widetilde{\omega}\widetilde{\tau}_1\vartheta} + \frac{i\overline{g}_{02}}{3\widetilde{\omega}}\overline{q}(0)e^{-i\widetilde{\omega}\widetilde{\tau}_1\vartheta} + E_1'e^{2i\widetilde{\omega}\widetilde{\tau}_1\vartheta}, \tag{4.20}$$

where $E_1' = (E_1^{(1)}, E_1^{(2)}) \in R^2$ is a constant vector. Similarly, from (4.16) and (4.19), we obtain

$$W_{11}(\vartheta) = -\frac{ig_{11}}{\widetilde{\omega}}q(0)e^{i\widetilde{\omega}\widetilde{\tau}_1\vartheta} + \frac{i\overline{g}_{11}}{\widetilde{\omega}}\overline{q}(0)e^{-i\widetilde{\omega}\widetilde{\tau}_1\vartheta} + E_2', \tag{4.21}$$

where $E_2' = (E_2^{(1)}, E_2^{(2)}) \in R^2$ is a constant vector. In what follows, we shall seek appropriate E_1 and E_2. From the definition of A and (3.16), we obtain

$$\int_{-1}^{0} d\eta(\vartheta)W_{20}(\vartheta) = 2i\widetilde{\omega}\widetilde{\tau}_1W_{20}(0) - H_{20}(0) \tag{4.22}$$

and

$$\int_{-1}^{0} d\eta(\vartheta)W_{11}(\vartheta) = -H_{11}(0), \tag{4.23}$$

where $\eta(\vartheta)=\eta(0,\vartheta)$. By (4.14), we have

$$H_{20}(0)=-g_{20}q(0)-\overline{g}_{02}\overline{q}(0)+2\widetilde{\tau}_1\begin{pmatrix}-\left(\frac{r}{k}e^{-i\widetilde{\omega}\widetilde{\tau}_1}+\alpha(1-m)q_1\right)\\ \theta\alpha(1-m)e^{-i\widetilde{\omega}\widetilde{\tau}_2}q_1\end{pmatrix} \tag{4.24}$$

and

$$H_{11}(0)=-g_{11}q(0)-\overline{g}_{11}\overline{q}(0)+2\widetilde{\tau}_1\begin{pmatrix}-\frac{r}{k}(e^{-i\widetilde{\omega}\widetilde{\tau}_1}+e^{i\widetilde{\omega}\widetilde{\tau}_1})-\alpha(1-m)Re\{q_1\}\\ \alpha(1-m)(\overline{q_1}e^{-i\widetilde{\omega}\widetilde{\tau}_2}+q_1e^{i\widetilde{\omega}\widetilde{\tau}_2})\end{pmatrix}. \tag{4.25}$$

Substituting (4.20) and (4.24) into (4.22) and noticing that

$$\left(i\widetilde{\omega}\widetilde{\tau}_1I-\int_{-1}^{0}e^{i\widetilde{\omega}\widetilde{\tau}_1\vartheta}d\eta(\vartheta)\right)q(0)=0$$

and

$$\left(-i\widetilde{\omega}\widetilde{\tau}_1I-\int_{-1}^{0}e^{-i\widetilde{\omega}\widetilde{\tau}_1\vartheta}d\eta(\vartheta)\right)\overline{q}(0)=0,$$

we obtain

$$\left(2i\widetilde{\omega}\widetilde{\tau}_1I-\int_{-1}^{0}e^{2i\widetilde{\omega}\widetilde{\tau}_1\vartheta}d\eta(\vartheta)\right)E_1'=2\widetilde{\tau}_1\begin{pmatrix}-\left(\frac{r}{k}e^{-i\widetilde{\omega}\widetilde{\tau}_1}+\alpha(1-m)q_1\right)\\ \theta\alpha(1-m)e^{-i\widetilde{\omega}\widetilde{\tau}_2}q_1\end{pmatrix}.$$

This leads to

$$\begin{pmatrix}2i\widetilde{\omega}-\frac{\alpha^2(1-m)^2hx^*y^*}{\{1+\alpha(1-m)hx^*\}^2}+\frac{rx^*}{k}e^{-i\widetilde{\omega}\widetilde{\tau}_1} & \frac{\alpha(1-m)x^*}{1+\alpha(1-m)hx^*}\\ -\frac{\theta\alpha(1-m)y^*e^{-i\widetilde{\omega}\widetilde{\tau}_2}}{\{1+\alpha(1-m)hx^*\}^2} & 2i\widetilde{\omega}\end{pmatrix}E_1'=2\begin{pmatrix}-\left(\frac{r}{k}e^{-i\widetilde{\omega}\widetilde{\tau}_1}+\alpha(1-m)q_1\right)\\ \theta\alpha(1-m)e^{-i\widetilde{\omega}\widetilde{\tau}_2}q_1\end{pmatrix}.$$

Therefore, it follows that

$$E_1^{(1)}=\frac{2}{A}\begin{vmatrix}-\left(\frac{r}{k}e^{-i\widetilde{\omega}\widetilde{\tau}_1}+\alpha(1-m)q_1\right) & \frac{\alpha(1-m)x^*}{1+\alpha(1-m)hx^*}\\ \theta\alpha(1-m)e^{-i\widetilde{\omega}\widetilde{\tau}_2}q_1 & 2i\widetilde{\omega}\end{vmatrix}$$

and

$$E_1^{(2)}=\frac{2}{A}\begin{vmatrix}2i\widetilde{\omega}-\frac{\alpha^2(1-m)^2hx^*y^*}{\{1+\alpha(1-m)hx^*\}^2}+\frac{rx^*}{K}e^{-i\widetilde{\omega}\widetilde{\tau}_1} & -\left(\frac{r}{k}e^{-i\widetilde{\omega}\widetilde{\tau}_1}+\alpha(1-m)q_1\right)\\ -\frac{\theta\alpha(1-m)y^*e^{-i\widetilde{\omega}\widetilde{\tau}_2}}{\{1+\alpha(1-m)hx^*\}^2} & \theta\alpha(1-m)e^{-i\widetilde{\omega}\widetilde{\tau}_2}q_1\end{vmatrix}.$$

where

$$A = \begin{vmatrix} 2i\widetilde{\omega} - \frac{\alpha^2(1-m)^2hx^*y^*}{\{1+\alpha(1-m)hx^*\}^2} + \frac{rx^*}{k} e^{-i\widetilde{\omega}\widetilde{\tau}_1} & \frac{\alpha(1-m)x^*}{1+\alpha(1-m)hx^*} \\ -\frac{\theta\alpha(1-m)y^* e^{-i\widetilde{\omega}\widetilde{\tau}_2}}{\{1+\alpha(1-m)hx^*\}^2} & 2i\widetilde{\omega} \end{vmatrix}.$$

Similarly, substituting (4.21) and (4.25) into (4.23), we get

$$\begin{pmatrix} -\frac{\alpha^2(1-m)^2hx^*y^*}{\{1+\alpha(1-m)hx^*\}^2} + \frac{rx^*}{k} & \frac{\alpha(1-m)x^*}{1+\alpha(1-m)hx^*} \\ -\frac{\theta\alpha(1-m)y^*}{\{1+\alpha(1-m)hx^*\}^2} & 0 \end{pmatrix} E_2' = 2 \begin{pmatrix} -\frac{r}{k}(e^{-i\widetilde{\omega}\widetilde{\tau}_1} + e^{i\widetilde{\omega}\widetilde{\tau}_1}) - \alpha(1-m)Re\{q_1\} \\ \alpha(1-m)(\overline{q_1}e^{-i\widetilde{\omega}\widetilde{\tau}_2} + q_1 e^{i\widetilde{\omega}\widetilde{\tau}_2}) \end{pmatrix}.$$

It follows that

$$E_2^{(1)} = \frac{2}{B'} \begin{vmatrix} -\frac{r}{k}(e^{-i\widetilde{\omega}\widetilde{\tau}_1} + e^{i\widetilde{\omega}\widetilde{\tau}_1}) - \alpha(1-m)Re\{q_1\} & \frac{\alpha(1-m)x^*}{1+\alpha(1-m)hx^*} \\ \alpha(1-m)(\overline{q_1}e^{-i\widetilde{\omega}\widetilde{\tau}_2} + q_1 e^{i\widetilde{\omega}\widetilde{\tau}_2}) & 0 \end{vmatrix}$$

and

$$E_2^{(2)} = \frac{2}{B'} \begin{vmatrix} -\frac{\alpha^2(1-m)^2hx^*y^*}{\{1+\alpha(1-m)hx^*\}^2} + \frac{rx^*}{K} & -\frac{r}{k}(e^{-i\widetilde{\omega}\widetilde{\tau}_1} + e^{i\widetilde{\omega}\widetilde{\tau}_1}) - \alpha(1-m)Re\{q_1\} \\ -\frac{\theta\alpha(1-m)y^*}{\{1+\alpha(1-m)hx^*\}^2} & \alpha(1-m)(\overline{q_1}e^{-i\widetilde{\omega}\widetilde{\tau}_2} + q_1 e^{i\widetilde{\omega}\widetilde{\tau}_2}) \end{vmatrix},$$

where

$$B' = \begin{vmatrix} -\frac{\alpha^2(1-m)^2hx^*y^*}{\{1+\alpha(1-m)hx^*\}^2} + \frac{rx^*}{k} & \frac{\alpha(1-m)x^*}{1+\alpha(1-m)hx^*} \\ -\frac{\theta\alpha(1-m)y^*}{\{1+\alpha(1-m)hx^*\}^2} & 0 \end{vmatrix}.$$

Thus, we can determine $W_{20}(\vartheta)$ and $W_{11}(\vartheta)$ from (4.20) and (4.21). Furthermore, g_{21} in (4.13) can be expressed by the parameters and delay. Thus, we can compute the following values:

$$\begin{aligned} c_1(0) &= \frac{i}{2\widetilde{\omega}\tau_{1_0}}(g_{20}g_{11} - 2|g_{11}|^2 - \frac{|g_{02}|^2}{3}) + \frac{g_{21}}{2}, \\ \mu_2 &= -\frac{\mathrm{Re}\{c_1(0)\}}{\mathrm{Re}\{\lambda'(\tau_{1_0})\}}, \\ \beta_2 &= 2\mathrm{Re}(c_1(0)), \\ T_2 &= -\frac{\mathrm{Im}\{c_1(0)\} + \mu_2 \mathrm{Im}\{\lambda'(\tau_{1_0})\}}{\widetilde{\omega}\tau_{1_0}}. \end{aligned}$$

which determine the qualities of bifurcating periodic solution in the center manifold at the critical value τ_{1_0}.

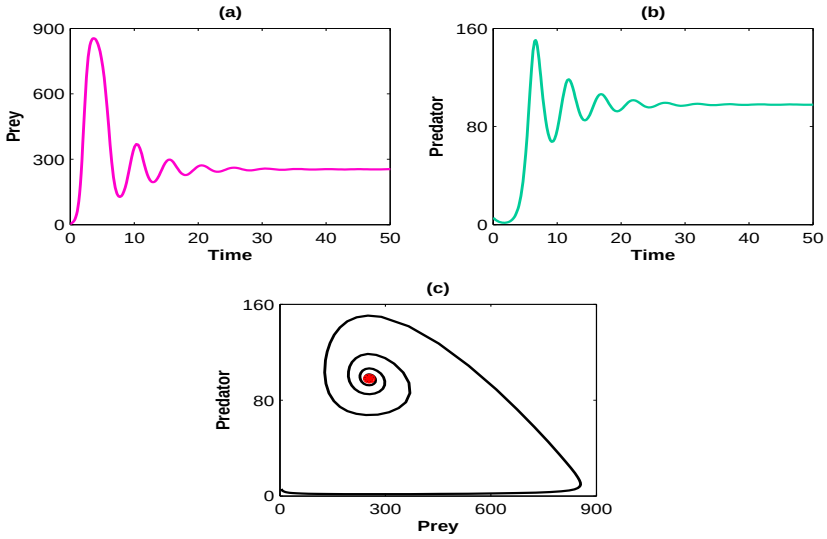

Figure 1: The coexistence equilibrium point $E^* = (253.9056, 97.8867)$ is locally asymptotically stable when $\tau_1 = 0 = \tau_2$. Figs. (a) and (b) are the time evolutions of the model system (1.3) and Fig. (c) is the corresponding phase plane.

Lemma 3.1 μ_2 determines the direction of the Hopf bifurcation. If $\mu_2 > 0$ ($\mu_2 < 0$) then the Hopf bifurcation is supercritical (subcritical) and the bifurcating periodic solutions exist for $\tau > \tau_{1_0}$ ($\tau < \tau_{1_0}$). β_2 determines the stability of the bifurcating periodic solutions: the bifurcating periodic solutions are stable (unstable) if $\beta_2 < 0$ ($\beta_2 > 0$). T_2 determines the period of the bifurcating periodic solutions: the period increases (decreases) if $T_2 > 0$ (< 0).

4 Simulation results

In this section, we give some numerical simulations to illustrate the analytical results observed in the previous sections. For illustration purpose, we consider the parameter values $r = 2.65,\ k = 898,\ \alpha = 0.045,\ m = 0.45,\ h = 0.0437,\ \theta = 0.215,\ d = 1.06$ with initial value $(30, 5.83)$.

The above parameter set satisfies all the conditions in Lemma 2.1 and

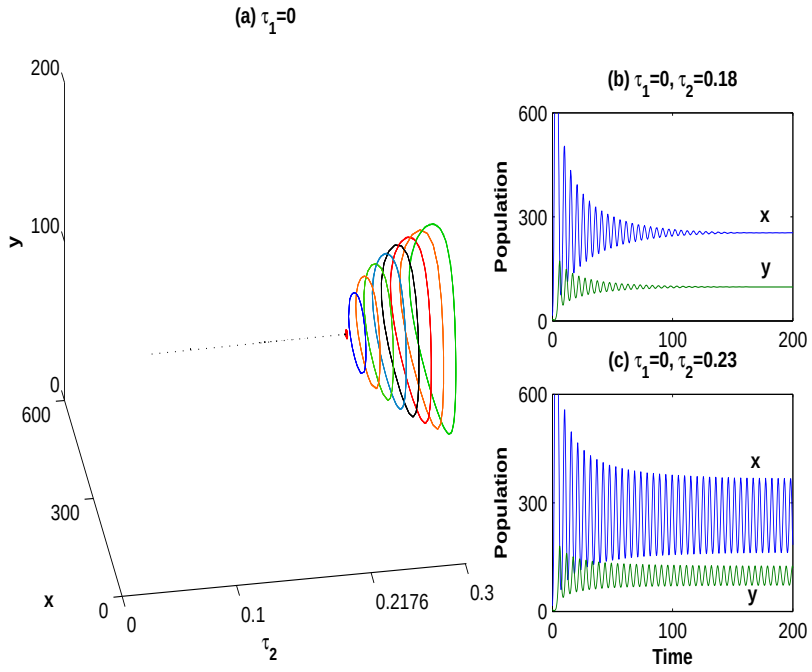

Figure 2: Bifurcation diagram (Figure 2(a))of system (1.3) with respect to the bifurcation parameter τ_2 is drawn in the three-dimensional space (τ_2, x, y) when $\tau_1 = 0$. Figure 2(b) shows the time evolution of the system when $\tau_2(= 0.18)$ is less than its critical value 0.2176. Figure 2(c) indicates the time evolution of the system when $\tau_2(= 0.23)$ is greater than its critical value 0.2176. These figures show that the coexistence equilibrium is stable for $\tau_2 < 0.2176$, unstable for $\tau_2 > 0.2176$ and Hopf-bifurcation occurs at $\tau = \tau_{2_0} = 0.2176$ with $\tau_1 = 0$.

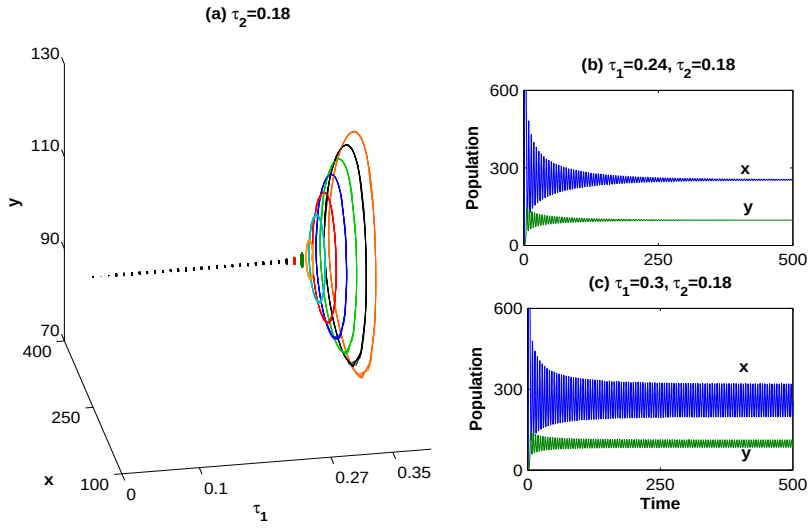

Figure 3: Bifurcation diagram (Figure 3(a))of system (1.3) with respect to the bifurcation parameter τ_2 is drawn in the three-dimensional space (τ_1, x, y) when $\tau_2 = 0.18$. Figure 3(b) shows the time evolution of the system when $\tau_1(= 0.24)$ is less than its critical value 0.27. Figure 3(c) indicates the time evolution of the system when $\tau_1(= 0.3)$ is greater than its critical value 0.27. These figures show that the coexistence equilibrium is stable for $\tau_1 < 0.27$, unstable for $\tau_1 > 0.27$ and Hopf-bifurcation occurs at $\tau = \tau_{1_0} = 0.27$ with $\tau_2 = 0.18$.

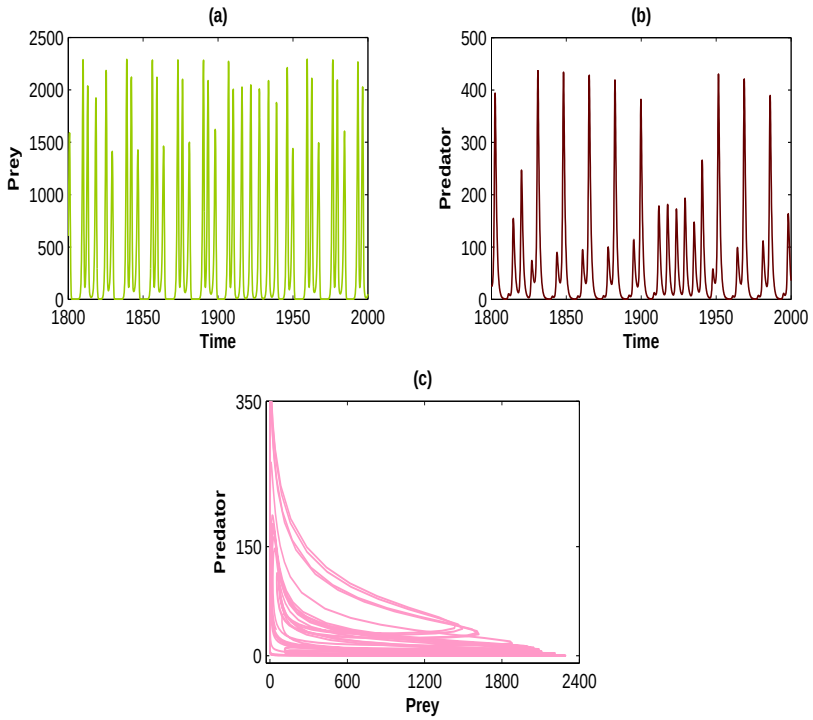

Figure 4: Irregular periodic behavior of the system (1.3) when $\tau_1 = 0.7$ ($> \tau_{1_0}$) and $\tau_2 = 0.8$ ($> \tau_{2_0}$). Figs. (a) and (b) are the time series of the prey and predator populations and Fig. (c) is the corresponding phase diagram.

consequently the system equation (1.3) converges to the coexistence equilibrium point $E^*(253.9056, 97.8867)$ when $\tau_1 = 0$, $\tau_2 = 0$ (Fig. 1). For the Case II, where $\tau_1 = 0$ and $\tau_2 \neq 0$, we compute $\omega_0 = 1.2345$ and $\tau_{2_0} = 0.2176$. Therefore, by Lemma 2.2, E^* is asymptotically stable for $\tau_2 < \tau_{2_0}$ and unstable for $\tau_2 > \tau_{2_0}$. The system experiences a Hopf bifurcation around E^* when $\tau_2 = \tau_{2_0}$. This behavior is depicted in the Fig. 2. Figure 2 (b-c) depict, respectively, that the system (1.3) is stable for $\tau_2 = 0.18$ ($< \tau_{2_0} = 0.2176$) and unstable for $\tau_2 = 0.23$ ($> \tau_{2_0} = 0.2176$) with $\tau_1 = 0$. The bifurcation diagram (Fig. 2(a)) clearly demonstrates the system behavior for different values of τ_2. It shows that the system remains stable if $\tau_2 < \tau_{2_0}$; but the instability sets in through periodic oscillations if $\tau_2 > \tau_{2_0}$. The system undergoes a Hopf bifurcation when $\tau_2 = \tau_{2_0} = 0.2176$. For the Case III, where $\tau_1 \neq 0$ and $\tau_2 \neq 0$, we vary τ_1 keeping the value of τ_2 within its stability range $(0, 0.2176)$. Choosing $\tau_2 = 0.18$, we obtain $\omega_1 = 1.1095$ as a root of the equation (2.7). In this case, the value of τ_{1_0} becomes 0.27 and the system (1.3) (following the Lemma 2.3) is locally stable (unstable) whenever $\tau_1 < 0.27$ (> 0.27). A Hopf bifurcation occurs when $\tau_1 = 0.27$. Fig. 3(b) shows that the system (1.3) is locally asymptotically stable for $\tau_1 = 0.24 < 0.27$; and Fig. 3(c) show that the system (1.3) is unstable for $\tau_1 = 0.3 > 0.27$. The bifurcation diagram (Fig. 3(a)) clearly demonstrates the system behavior for different values of τ_1. In Case IV, when $\tau_2 = 0, \tau_1 \neq 0$, one can compute $\bar{\omega}_0 = 1.6095$ and the corresponding critical value of τ_1 as $\tau_{1_0} = 0.6167$. Therefore, the coexistence equilibrium $E^*(x^*, y^*)$ is locally asymptotically stable for $\tau_1 < \bar{\tau}_{1_0} = 0.6167$ and it is unstable for $\tau_1 > \bar{\tau}_{1_0} = 0.6167$. Similarly for Case V, we take any value of τ_1 from its stability range $[0, 0.6167)$, say $\tau_1 = 0.45$, and consider τ_2 as a free parameter. One finds that $\bar{\omega}_1 = 1.6468$ and the corresponding critical value of τ_2 is $\bar{\tau}_{2_0} = 0.091$. Thus, for any fixed stable value of τ_1, the system exhibits stable behavior around $E^*(x^*, y^*)$ for $\tau_2 < \bar{\tau}_{2_0}$ and unstable oscillatory behavior for $\tau_2 > \bar{\tau}_{2_0}$.

Using Lemma 3.1, one can determine the values of $c_1(0), \mu_2, \beta_2$ and T_2 as $c_1(0) = -0.000069936 - 0.00046189i$, $\mu_2 = 0.000033112 (> 0)$, $\beta_2 = -0.000013987$ (< 0) and $T_2 = 0.000023056 (> 0)$. Since $\mu_2 > 0$ and $\beta_2 < 0$, the Hopf bifurcation is supercritical and stable. Also, the period of the bifurcating periodic solutions increases with τ_1 (as $T_2 > 0$), where τ_2 is kept fixed in its stable region.

So far we have observed the behavior of the system when the delay pa-

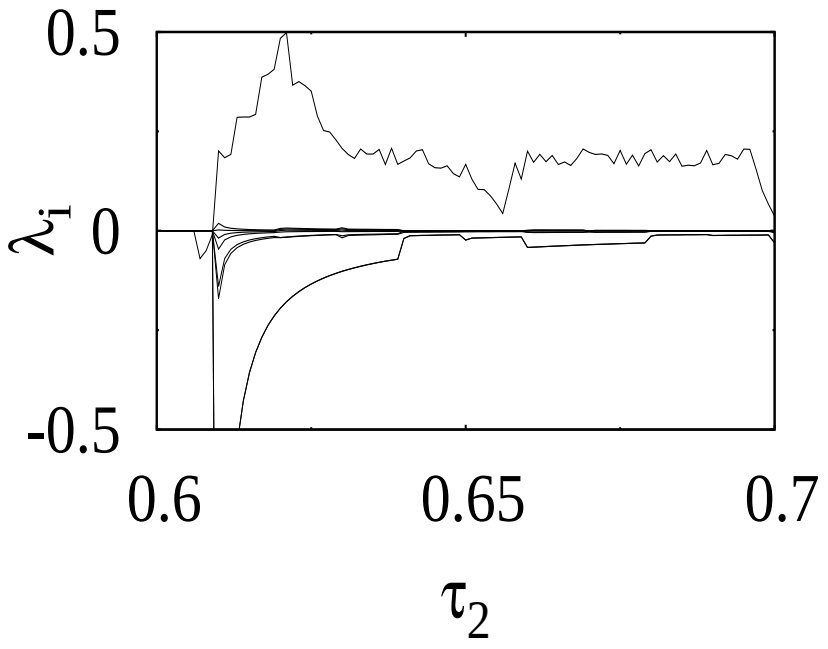

Figure 5: Lyapunov exponents test of the chaotic solutions of the system (1.3). Parameters are as in the Fig. 4. Here the largest few exponents have been plotted as a function of τ_2. The highest one, namely λ_1 is positive for a large range of τ_2 indicating chaos.

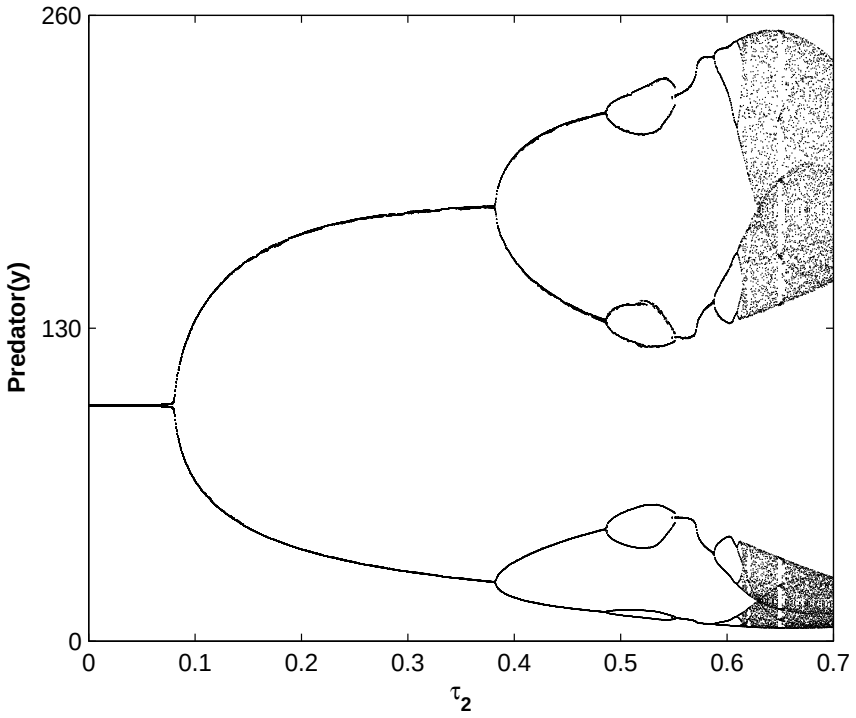

Figure 6: Bifurcation diagram of the predator population when the delay parameter τ_2 is smoothly varied with fixed $\tau_1 = 0.5$. Other parameters are as in Figure 1.

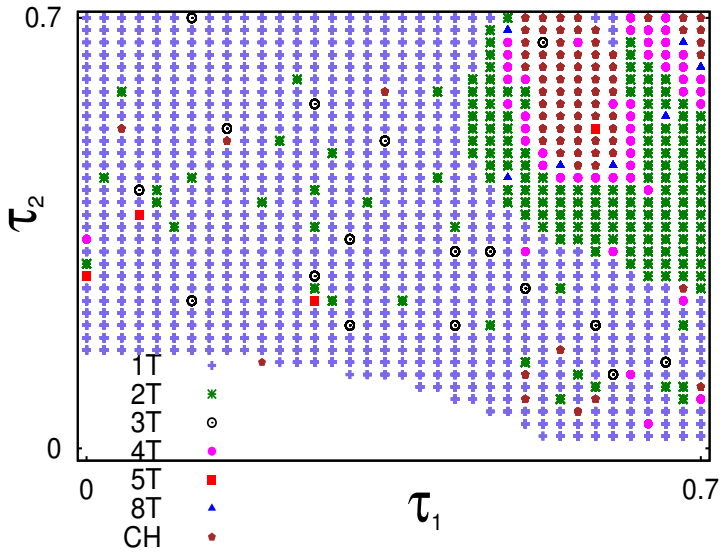

Figure 7: Stability regions of the system (1.3) are depicted in the $\tau_1\tau_2$-plane for fixed m ($= 0.45$). Different dynamical features are depicted by different indices which are given in the figure. Remaining parameters are as in the Figure 1.

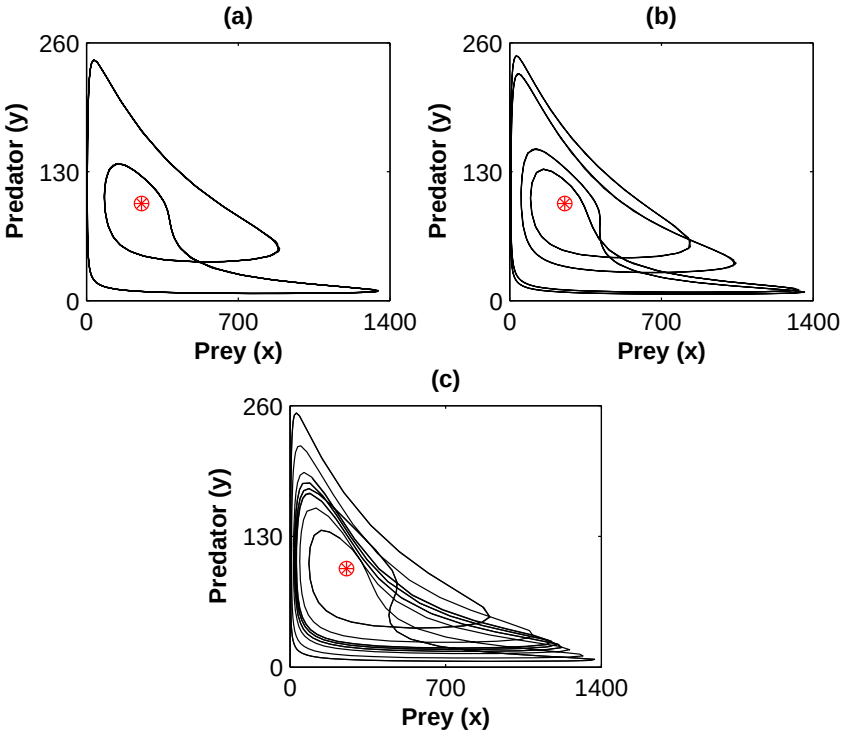

Figure 8: nT periodic solution of the system (1.3) with different τ_2 ($> \tau_{2_0}$) but fixed τ_1 ($> \tau_{1_0}$). (a) 2T period: $\tau_1 = 0.5, \tau_2 = 0.56$, (b) 4T period: $\tau_1 = 0.5, \tau_2 = 0.6$ and (c) 8T period: $\tau_1 = 0.5, \tau_2 = 0.6$. Other parameters are as in Table 1.

rameters are within or slightly above the critical values. One interesting topic in the delay-induced system is to study the dynamical behavior of the system when the delay parameters are far away from their critical values, or they assume large values. To observe the dynamics, we have simulated our model system (1.3) for larger values of τ_1 and τ_2.

Our simulation results indicate that the system exhibits irregular periodic behaviors for $\tau_1 = 0.7$ ($> \tau_{1_0}$) and $\tau_2 = 0.8$ ($> \tau_{1_0}$) (Fig. 4). In order to characterize this irregular behavior, we perform the standard numerical diagnostics of the solutions, viz., Lyapunov exponents. Lyapunov exponent or Lyapunov characteristic exponent of a dynamical system is a quantity that characterizes the rate of separation of infinitesimally close trajectories. Neg-

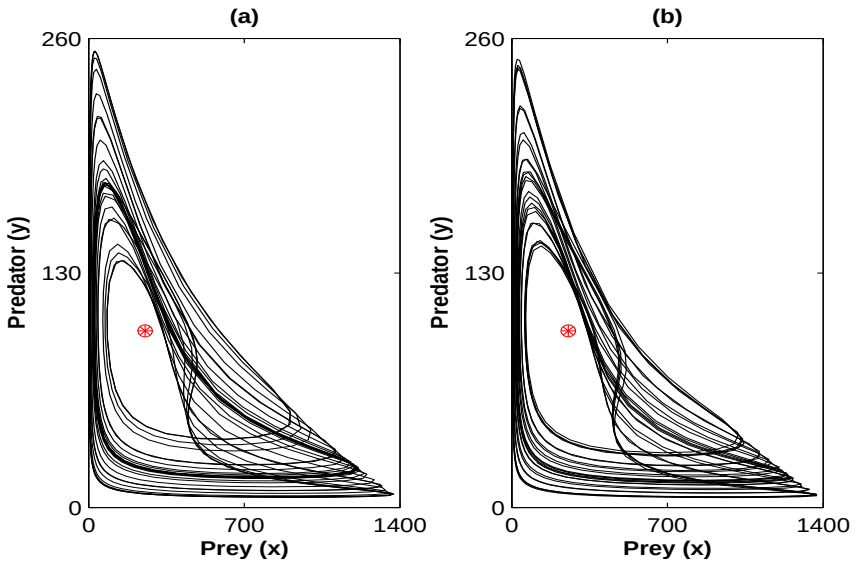

Figure 9: The system (1.3) exhibits chaotic dynamics for $\tau_2 = 0.626$ (Fig. (a)) and $\tau_2 = 0.66$ (Fig. (b)). Other parameters are as in the Fig. 9.

ative, zero and positive Lyapunov exponents (λ) indicate, respectively, the stable, unstable and chaotic behavior of the system. For the parameter values as in the Fig. 4, the value of the largest Lyapunov exponent (λ) is found to be positive when τ_2 varies, indicating chaotic dynamics of the system (1.3) (Fig. 5).

In Fig. 6, we have shown a typical bifurcation diagram of the predator population y for fixed $\tau_1 = 0.5$ and variable τ_2. The bifurcation diagram shows that the system (1.3) exhibits a rich dynamics such as period-doubling bifurcation, period-halving bifurcation, chaotic band, narrow windows, etc. as the parameter τ_2 is smoothly varied. To observe the interplay between the strength of delay parameters, we have plotted the stability region of the system (1.3) in the $\tau_2\tau_1$-plane for a fixed value of $m = 0.45$ (Fig. 7). This figure indicates that the two delays follow inverse relationship for maintaining the stability of the system. However, if the delays are large then the system is always chaotic. Different dynamical features like stable equilibrium, different nT-periodic solutions and chaotic dynamics are clearly depicted by different indices in this figure. The phase-space of the system (1.3) for different τ_2 ($> \tau_{2_0}$) but fixed τ_1 ($> \tau_{1_0}$) shows that the system exhibits T-period solu-

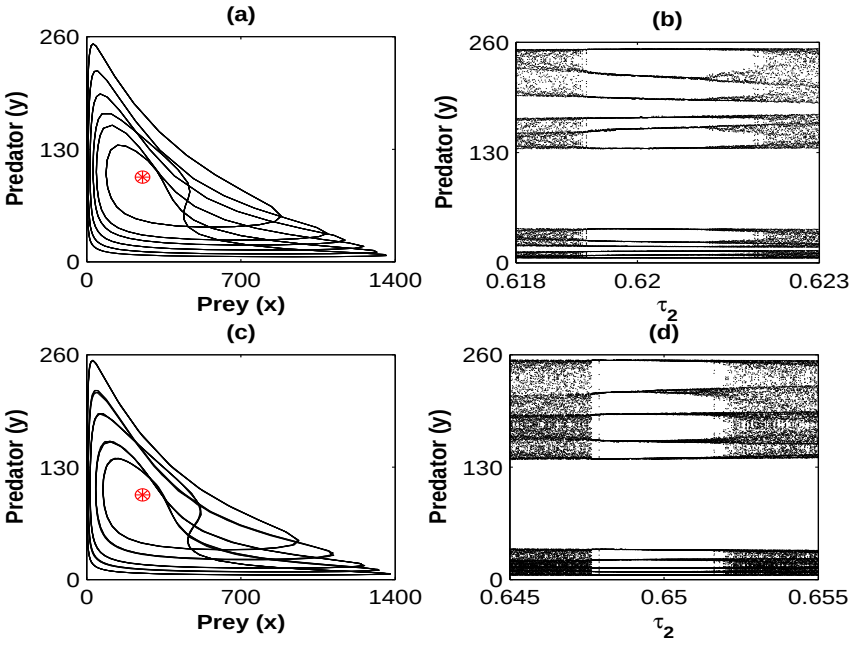

Figure 10: The system (1.3) exhibits $6T-$period solutions for $\tau_2 = 0.62$ (Fig. (a)) and $5T-$period solutions for $\tau_2 = 0.65$ (Fig. (c)). Magnified parts of the Fig. 6 over [0.618, 0.623] (Fig. (b)) and [0.645, 0.655] (Fig. (d)). Other parameters are as in the Fig. 4.

tion for $\tau_2 = 0.3$, $2T$-period solution for $\tau_2 = 0.4$ and $4T$-period solution for $\tau_2 = 0.53$ (Fig. 7). The system shows period-halving for $\tau_2 = 0.56$ and again period-doubling at $\tau_2 = 0.6$ and $\tau_2 = 0.626$ (Fig. 8). The system exhibits chaotic dynamics for $\tau_2 = 0.63$ and $\tau_2 = 0.66$ (Fig. 9). The system again shows $6T$-period solution for $\tau_2 = 0.62$ (Fig. 10(a)) and $5T$-period solution for $\tau_2 = 0.65$ (Fig. 10(c)). Periodic windows are intermittently scattered. The magnified periodic windows over the values of $\tau_2 = [0.618, 0.623]$ and $\tau_2 = [0.645, 0.655]$ are shown in Fig. 10(b) and Fig. 10(d), respectively.

5 Summary

Effect of prey refuge has not been considered explicitly in the prey-predator models. However, both field and laboratory experiments confirm that prey refuge reduces predation rates by decreasing encounter rates between predator and prey. On the other hand, a prey-predator model becomes more realistic in the presence of different delays which are unavoidable elements in physiological and ecological processes. In this paper, a prey-predator model that incorporates different biological delays and the effect of prey refuge is studied. A time delay τ_1 is considered in the logistic prey growth rate to represent density dependent feedback mechanism and the second time delay τ_2 is considered in the predator response function to represent its gestation delay. The objective is to study the dynamic behavior of a multi-delayed prey-predator system in the presence of prey refuge.

It is observed that the non-delayed system is asymptotically stable under some parametric restrictions. There is a critical value (τ_{2_0}) of the gestation delay parameter (τ_2), below which the single-delayed system ($\tau_1 = 0$) is locally asymptotically stable and above which the system is unstable. A Hopf-bifurcation occurs when the delay parameter attains the critical value τ_{2_0}. Keeping gestation delay (τ_2) within its stability range, a critical value τ_{1_0} of the negative feedback mechanism delay parameter (τ_1) is obtained below which the double-delayed system is locally stable and above which the system is unstable. A Hopf-bifurcation occurs at $\tau_1 = \tau_{1_0}$. Similarly, if we first keep $\tau_2 = 0$, we get previous type result from this system. The system exhibits irregular behavior when these delays are large and above their critical values. This irregularity has been identified as chaotic through different tests. These simulations indicate that the system exhibits a rich dynamics such as period-

doubling bifurcation, period-halving bifurcation, chaotic band, narrow and wide windows etc as the parameter τ_2 is smoothly varied. It is also observed that the strength of the prey refuge increases with delays to keep the system in stable condition. The inter-play between two delays for fixed value of prey refuge has also been determined. It is noticed that these delays work in a complementary fashion. In other words, to keep the system in stable condition, the delay in the logistic prey growth should be low when gestation delay is high or vice versa. Thus, a prey-predator system may exhibit simple stable behavior, regular cyclic behavior or chaotic behavior depending on the length of delays.

Acknowledgment
M. Lakshmanan acknowledges National Academy of Sciences, India for financial support in the form of a Senior Scientist Platinum Jubilee Fellowship.

References

1. Alstad, D., 2001. Basic Populations Models of Ecology. Prentice Hall, Inc., NJ.

2. Anderson, O., 1984. Optimal Foraging by largemouth bass in structured environments. Ecology, 65, 851-861.

3. Anderson, T. W., 2001. Predator responses, prey refuges and density-dependent mortality of a marine fish. Ecology, 82(1), 245-257.

4. Johnson, W.D., 2006. Predation, habitat complexity and variation in density dependent mortality of temperate reef fishes. Ecology, 87(5), 1179-1188.

5. Jana, D., Ray, S., 2016. Impact of physical and behavioral prey refuge on the stability and bifurcation of Gause type Filippov prey-predator system. Model. Earth Syst. Environ. 2-24.

6. Lima, S. L. and L. M. Dill., 1990. Behavioral decisions made under the risk of predation - a review and prospectus. Canadian Journal of Zoology. 68, 619-640.

7. Bell, S. S., E. D. McCoy, and H. R. Mushinsky., 1991. Habitat structure: the physical arrangement of objects in space. Chapman and Hall, New York, New York, USA.

8. Lima, S. L. 1998. Stress and decision making under the risk of predation: recent developments from behavioral, reproductive, and ecological perspectives. Advances in the Study of Behavior. 27, 215-290.

9. Brown, J. S. and B. P. Kotler. 2004. Hazardous duty pay and the foraging cost of predation. Ecology Letters. 7, 999-1014.

10. Caro, T. 2005. Anti predator defenses in birds and mammals. University of Chicago Press, Chicago, Illinois, USA.

11. Stankowich, T., and D. T. Blumstein. 2005. Fear in animals: a meta-analysis and review of risk assessment. Proceedings of the Royal Society Series B. 272, 2627-2634.

12. Cooper, W. E., Jr. 2009. Theory successfully predicts hiding time: new data for the lizard Sceloporus virgatus and a review. Behavioral Ecology. 20, 585-592.

13. Luckinbill LS. Coexistence in Laboratory Populations of *Paramecium aurelia* and its predator *Didinium nasutum*. Ecology 1973; 54: 1320-1327.

14. Sih A. et al. Predation, competition, and prey communities, a review of field experiments. Annual Review of Ecology and Systematics 1985; 16: 269-311.

15. Ray, S., Straškraba, M., 2001. The impact of detritivorous fishes on the mangrove estuarine system. Ecological Modeling, 140, 207-218.

16. Roy, M., Mandal, S., Ray, S., 2008. Detrital ontogenic model including decomposer diversity. Ecological Modeling, 215, 200-206.

17. Savino JF, Stein RA. Predator-prey interaction between largemouth bass and bluegills as influenced by simulated, submersed vegetation. Trans American Fisheries Soci. 1982; 111: 255-266.

18. Kar T. K. Stability analysis of a preypredator model incorporating a prey refuge, Communication in Nonlinear Science and Numerical Simulation, 10: 681691, 2005.

19. Jana, D., 2013. Chaotic dynamics of a discrete predator-prey system with prey refuge. Applied Mathematics and Computation. 224, 848-865.

20. Jana, D., 2014. Stabilizing Effect of Prey Refuge and Predator's Interference on the Dynamics of Prey with Delayed Growth and Generalist Predator with Delayed Gestation. International Journal of Ecology. Volume 2014, Article ID 429086, 12 pages. doi.org/10.1155/2014/429086.

21. Jana, D., Agrawal, R. and Upadhyay, R. K., 2015. Dynamics of generalist predator in a stochastic environment: effect of delayed growth and prey refuge. Applied Mathematics and Computation. 268, 1072-1094.

22. Bairagi N, Jana D. On the stability and Hopf bifurcation of a delay-induced predator-prey system with prey refuge. Applied Mathematical Modelling 2011; 35: 3255-3267.

23. Jana, D., Agrawal, R. and Upadhyay, R. K., 2014. Top-predator interference and gestation delay as determinants of the dynamics of a realistic model food chain. Chaos, Solitons & Fractals. 69, 50-63.

24. Rosenzweig ML, MacArthur RH. Graphical representation and stability conditions of predator-prey interactions. American Naturalist 1963; 47: 209-223.

25. MacDonald M. Biological Delay Systems: Linear Stability Theory, Cambridge University Press, Cambridge; 1989.

26. May RM. Theoretical ecology: principles and applications. Blackwell Scientific Publications, Oxford; 1981.

27. Xiao D, Ruan S. Multiple bifurcations in a delayed predator-prey system with nonmonotonic functional response. J. Differential Equ 2001; 176: 494-510.

28. Yan XP, Chu YD. Stability and bifurcation analysis for a delayed Lotka-Volterra predatorprey system. J. Comp. Appl. Maths 2006; 196: 198-210.

29. Song Y, Peng Y, Wei J. Bifurcations for a predatorprey system with two delays. J. Math. Anal. Appl. 2008; 337: 466-479.

30. Nakaoka S, Saito Y, Takeuchi Y. Stability, delay, and chaotic behavior in a Lotka-Volterra predator-prey system. Math. Biosci. Enginee 2006; 3: 173-187.

31. Xu C, Liao M, He X. Stability and Hopf bifurcation analysis for a Lotka-Volterra predator-prey model with two delays. Int. J. Appl. Math. Comput. Sci. 2011; 21(1): 97-107.

32. Liao M, Tang X, Xu C. Bifurcation analysis for a three-species predatorprey system with two delays. Commun Nonlinear Sci Numer Simulat 2012; 17: 183-194.

33. D. Jana, R. Pathak, M. Agarwal, On the stability and Hopf bifurcation of a prey-generalist predator system with independent age-selective harvesting. Chaos, Solitons & Fractals. 83 (2016) 252-273.

34. Yang R., Wei J. Stability and bifurcation analysis of a diffusive prey-predator system in Holling type III with a prey refuge. Nonlinear Dynamics. 2014; 79(1): 631-646.

35. Yang R., Zhang C. Dynamics in a diffusive predator-prey system with a constant prey refuge and delay. Nonlinear Analysis Real World Application. 2016; 31: 1-22.

36. Yang R., Zhang C. The effect of prey refuge and time delay on a diffusive predator-prey system with hyperbolic mortality. Complexity. 2016; 50(3): 105-113.

37. Freedman, HI. Deterministic Mathematical Models in Population Ecology. HIFR Consulting Ltd., Edmonton; 1987.

38. Kuang, Y. Delay Differential Equations with Applications in Population Dynamics. Academic Press, New York; 1993.

39. Butler, G., Freedman, H. I. and Waltman, P. Uniformly persistent systems. Proceedings of American Mathematical Society. 1986; 96(3): 425-430.

40. Freedman, H. I. and Waltman, P. Persistence in models of three interacting predator-prey populations. Math. Biosci. 1984; 68: 213-231.

41. Freedman, H. I. and SO, J. Global stability and persistence of simple food chains. Math. Bios. 1985; 76: 69-86.

42. Brauer F., Chavez C.C., 2001. Mathematical models in population biology and epidemiology, Springer, New York.

43. Gaurd, T. C. and Hallam, T. G. Persistence in food web-I, Lotka-Voltera chains. Bulletin of Mathematical Biology. 1979; 41: 877-891.

44. X. Yang, L. Chen, J. Chen, Permanence and positive periodic solution for the single species nonautonomous delay diffusive model, Compu. Math. App. 32 (1996) 109-116.

45. Ruan S, Wei J. On the zeros of transcendental functions with applications to stability of delay differential equations. Dynam. Contin. Discr. Impuls. Syst 2003; 10: 863-874.

46. Hassard BD, Kazarinoff ND, Wan, YH. Theory and Application of Hopf Bifurcation, Cambridge University, Cambridge; 1981.

47. Gopalsamy K, He X. Delay-independent stability in bi-directional associative memory networks. IEEE Trans. Neural Netw. 1994; 5: 998-1002.

48. Butzel HM, Bolten AB. The relationship of the nutritive state of the prey organism *Paramecium aurelia* to the growth and encystment of *Didinium nasutum*. J. Protozo. 1968; 15: 256-258.

49. Harrison GW. Comparing predator-prey models to Luckinbill's experiment with Didinium and Paramecium. Ecology 1995; 76(2): 357-374.

50. Jost C, Ellner SP. Testing for predator dependence in predator-prey dynamics: a non-parametric approach, Proc. R. Soc. Lond. B 2000; 267: 1611-1620.

51. Persson L. Behavioral response to predators reverses the outcome of competition between prey species. Behavioral Ecology and Sociobio. 1991; 28: 101-105.

52. Reukauf E. Zur biologie *von Didinium nasutum*. Zeitschrift fur vergleichende Physiologie 1930; 11: 689-701.

53. Salt GW. Predator and prey densities as controls of the rate of capture by the predator *Didinium nasutum*. Ecology 1974; 55: 434-439.